1 **Title Page**

2

Full title Adult porcine (*Sus scrofa*) derived inner ear cells possessing multipotent stem/progenitor cell characteristics in *in vitro* cultures

Short title Adult porcine derived inner ear *in vitro* cell culture

Authors& Affiliations

1) Printha Wijesinghe

[1]Division of Otolaryngology, Department of Surgery, University of British Columbia, Vancouver, British Columbia, Canada

[2]Vancouver Coastal Health Research Institute, Vancouver, British Columbia, Canada

Email: printha.wijesinghe@ubc.ca

2) Anand Sastry

[1] Consultant Interventional Neuroradiologist, University Hospital of Wales, United Kingdom

Email: Anand.Sastry@wales.nhs.uk

3) Elizabeth Hui

[1]Division of Otolaryngology, Department of Surgery, University of British Columbia, Vancouver, British Columbia, Canada

[2]Vancouver Coastal Health Research Institute, Vancouver, British Columbia, Canada

Email: ehui@cmmt.ubc.ca

4) Tristan A. Cogan

[1]Bristol Veterinary School, University of Bristol, Langford House, Langford, Bristol, United Kingdom

Email: tristan.cogan@bristol.ac.uk

5) Boyuan Zheng

[1]Division of Otolaryngology, Department of Surgery, University of British Columbia, Vancouver, British Columbia, Canada

[2]Vancouver Coastal Health Research Institute, Vancouver, British Columbia, Canada

Email: boyuanzheng94@gmail.com

6) Germain Ho

[1]Division of Otolaryngology, Department of Surgery, University of British Columbia, Vancouver, British Columbia, Canada

[2]Vancouver Coastal Health Research Institute, Vancouver, British Columbia, Canada

Email: germain.ho@hotmail.com

7) Juzer Kakal

[1]Division of Otolaryngology, Department of Surgery, University of British Columbia, Vancouver, British Columbia, Canada

[2]Vancouver Coastal Health Research Institute, Vancouver, British Columbia, Canada

Email: jk.consulting.canada+pubs@gmail.com

8) Desmond A. Nunez

[1]Division of Otolaryngology, Department of Surgery, University of British Columbia, Vancouver, British Columbia, Canada

[2]Vancouver Coastal Health Research Institute, Vancouver, British Columbia, Canada

[3]Division of Otolaryngology, Head & Neck Surgery, Gordon &

Leslie Diamond Health Care Centre, Vancouver General Hospital, Vancouver, British Columbia, Canada

Email: desmond.nunez@ubc.ca

Corresponding Author Desmond A Nunez MD MBA FRCS(ORL) FRCSC

Associate Professor, Head- Division of Otolaryngology,

Department of Surgery,

The University of British Columbia, Diamond Health Care Centre

4th Floor-2775 Laurel Street, Vancouver, BC Canada V5Z 1M9

Email: desmond.nunez@ubc.ca

Phone: 604 875 4664

Fax: 604 875 5018

ORCID ID: 0000-0002-7501-9625

Abstract

The human inner ear compared with that of other mammalian species is very complex. Although the mouse's cochlea is frequently studied the mouse's inner ear continues to develop postnatally whilst the human inner ear is fully developed by the third month of gestation which leads one to question the applicability of findings based on research on mice to human regenerative therapies. Here, we report a novel *in vitro* culture of adult porcine (*Sus scrofa*) inner ear cells developed from post-mortem labyrinth specimens. Anatomical findings based on maximal transverse and vertical axial diameters and the length of the cochlear duct suggest that the pig's cochlea is similar to the human cochlea. *In vitro* cultures of porcine cochlear and vestibular cells showed the persistence of both inner ear hair cell (HC), supporting cell (SC) and stem/progenitor cell characteristics across passages up to 6 based on scanning electron microscopy, fluorescence immunocytochemistry and quantitative reverse transcription polymerase chain reaction (RT-qPCR). Our findings showed that porcine cochlear and vestibular epithelia maintained multipotent stem/progenitor cell populations into adulthood although their regenerative capacities differed across the passages. The development of a viable and reproducible method to culture porcine inner ear cells provides an important investigative tool that can be utilized to study and evaluate the pathophysiological causes and cellular consequences of human inner ear disorders.

Keywords: Porcine inner ear anatomy, *in vitro* cell culture, cellular characterizations, multipotent stem/progenitor cells

Introduction

Human hearing and balance disorders are mostly attributed to damage to the mechanosensory hair cells (HCs) of the cochlear and vestibular sensory epithelia, respectively. These HCs are susceptible to a variety of insults including noise, ototoxic compounds, ageing and the interaction of adverse environmental and genetic factors [1]. Regardless of the cause, lost or damaged human cochlear HCs are never replaced, and the replacement of vestibular HCs occurs at levels too low to support significant functional recovery [2, 3]. In mammals, sensory HCs arise from embryonic progenitor cells during the embryonic period and in some species such as mice where the ear is not fully developed at birth, also during the early post-natal period [4]. There is as yet no evidence of newly generated *de-novo* mammalian auditory HCs in the mature cochlea [5].

Mammalian vestibular HC regeneration is believed to arise through nonmitotic trans-differentiation of supporting cells (SCs) [6, 7]. In contrast to mammals, non-mammalian vertebrates such as birds produce or regenerate auditory HCs after trauma, and thus can maintain optimum hearing function throughout their lives [8]. The observed patterns of cell division and differentiation in avian species suggest that their HCs regenerate from postembryonic progenitor cells [9]. The generation of new HCs from a renewable source of progenitor cells is a principal requirement for the development of an inner ear cell-based therapy [10].

The study of human HCs is severely limited because the cochlea is technically difficult to access, tissue harvest leads to severe and permanent hearing disability, and surgery involving inner ear tissue removal is comparatively rare. Hence other species are utilized in mammalian inner ear research. The mouse is the most commonly studied species due to its

small size, high reproductive rate, large reported genetic database, variety of different strains, and the relatively low cost to procure and maintain study subjects. However, the mouse's inner ear continues to develop postnatally whilst the human inner ear is fully developed by the third month of gestation [4] meaning that mice retain the capacity for auditory sensory HC regeneration after birth in contrast to humans which questions the applicability of findings based on research on mice to human regenerative therapies.

The pig has been considered as a superior model for the study of human diseases particularly for understanding complex conditions such as obesity, arthritis, cardiovascular, skin, and eye diseases [11]. Pigs have many similarities to human with respect to compatible organ size, immunology and physiological functions. Their high-quality annotated reference genome sequence and many known alleles presumed to cause diseases extend the potential of the pig as a biomedical study model [12, 13]. The morphology and the development of the inner ear of miniature pigs have been reported to be similar to that of humans [14].

Our objectives were to develop a viable method to isolate porcine inner ear cells from postmortem cochlear and vestibular epithelia, document the porcine inner ear anatomical structure, and report an *in vitro* mixed cell culture model that demonstrated the presence and persistence of inner ear HC, supporting cell (SC) and stem/progenitor cell characteristics.

Materials and Methods

Ethical Approval

This study was approved by the Biosafety Committee of the University of British Colombia (B14-0048, B18-0048), Vancouver, Canada and by the Animal Research Ethics Review, University of Bristol, Bristol, United Kingdom. All the experiments were performed in accordance with host institutional Policies and Procedures, Biosafety Practices and Public Health Agency of Canada guidelines as required.

Tissue harvest, isolation and cell culture

Twenty-four temporal bone labyrinth capsules were harvested from 12 adult pigs (*Sus scrofa*) with ages ranging from 15-19 weeks. Six temporal bone labyrinths were selected at random for identification of the gross anatomy and histological study. The otic capsule of the temporal bones were isolated from euthanized adult pigs immediately post-mortem (within 2 hours) and placed in pre-chilled sterile Dulbecco's phosphate-buffered saline (DPBS).

Four temporal bone labyrinths were used for *in vitro* cell cultures. The helicotrema of the cochlea was opened and the cochlear duct-extracted piecemeal. Vestibular tissue was harvested in part via the oval window, and by dissection of the bony semi-circular canals with special attention to harvesting darkly pigmented vestibular epithelium.

The harvested tissues were macerated under a dissection microscopic vision, keeping the cochlear and vestibular tissues separate. Each cochlear and vestibular tissues were collected in separate 15ml sterile tubes contaning 10ml DPBS and 2ml of 0.25% trypsin-EDTA and then incubated at 37^{o}C for 20-25 minutes for trypsiniation. Tissues extracted from two

112 temporal bone labyrinths were preserved separately in RNAlater, a protective reagent, and
113 stored at -80^{o}C for subsequent RNA extraction.
114
115 Following incubation, the tubes were centrifuged at 300 x g for 5minutes and the resulting
116 cell pellets were re-suspended in 3ml of growth medium consisting of Dulbecco's Modified
117 Eagle Medium (DMEM) enriched with 10% Fetal Bovine Serum (FBS). About 500µl of the
118 cellular suspension was then placed into each well of a 6-well cell culture plate pre-filled
119 with 1.5ml of fresh growth medium.
120
121 The culture plate was placed into an incubator set at 37^{o}C and 5%CO_2. Half of the medium
122 was replaced after a week taking care not to disturb the growing cells, and after a further 5-7
123 days all the medium was changed. When the cell growth reached >80% confluence
124 (approximately 3 weeks), the cells were washed with DPBS buffer and trypsinized using
125 250µl of 0.25% trypsin-EDTA per well and incubated at 37^{o}C for 5 minutes. Trypsinization
126 was stopped by adding 9 ml of DMEM medium (without 10% FBS) and the pooled
127 suspension was centrifuged at 300 x g for 5minutes. One-third portion of the cell pellet
128 (passage 0 or P0) was re-suspended in fresh growth medium and placed in T_{25} vented culture
129 flasks. The next generation of cells (passage 1 or P1 cells) was allowed to grow until >80%
130 confluence was reached.
131
132 The cells were subsequently re-passaged again, up to P6, allowing for >80% confluence
133 before each passage. The morphology of the cochlear and vestibular derived cells were
134 recorded at each passage by a Phase-contrast Zeiss Axio Vert.A1 inverted microscope. Ultra-
135 morphological features were obtained by a Scanning Electron Microscope (SEM) - Hitachi
136 S4700 on passaged cells.

We have used House Ear Institute-Organ of Corti 1 (HEI-OC1) cells (gifted by Dr. F. Kalinec), a conditionally immortalized mouse auditory cell line as a positive control for cellular characterization studies [15]. HEI-OC1 cells were cultured under non-permissive conditions by incubating at 37^{o}C and 5% CO_2 in T_{25} vented culture flasks containing DMEM medium and 10% FBS without supplements.

Scanning electron microscopy on passaged inner ear cell cultures

Ultra-morphological features of P4 passaged porcine inner ear cells and HEI-OC1 cells were obtained by scanning electron microscopy. The porcine inner ear cells and HEI-OC1 cells were grown on poly-L-lysine coated cover slips under the above described culture conditions. At 100% confluence, cells were prepared for SEM [16] as follows: cells were washed using straight phosphate buffer (pH 7.4) and fixed for 30 minutes with 2.5% glutaraldehyde in 0.1 M sodium cacodylate buffer (pH 7.4), containing 2mM $CaCl_2$. After fixation, cells were washed 3 times with 0.1M sodium cacodylate buffer (pH 7.4), each for 1 minute, post-fixed for 10-15 minutes with 1% osmium tetroxide (OsO4) in the same sodium cacodylate buffer and then washed. The cells were progressively dehydrated in a graded ethanol series, critical point-dried using CO_2 and sputter-coated with gold/palladium (Au/Pd). The cells were then examined using a Hitachi S4700 SEM.

Temporal bone sectioning, histology and inner ear anatomy

The bone labyrinths of six temporal bones were obtained as described above and fixed in 37% formaldehyde. The diameters of the six labyrinthine bones were measured with precision digital calipers. The bones were then decalcified by first immersing in 0.5M EDTA (pH 8.0) solution for 7 days. This was re-freshed with 0.5M EDTA (pH 8.0) solution for a

minimum of four times over the 7 days. The bones were then immersed in 10% sucrose for 2 hours, followed by 20% sucrose for 24 hours and 30% sucrose for 24 hours. Four of the bones were then placed in an optimum cutting temperature (OCT) medium at room temperature.

A round window cochleostomy was fashioned under microscopic control in two of the cochleas. The length of the cochlea was determined by observing how far the active electrode array of a standard Nucleus 22 cochlear implant could be inserted via the round window.

All of the decalcified specimens embedded in OCT were frozen in isopentane held in the vapour phase of liquid nitrogen. Serial 5μm sections of the bones were cut with a microtome and placed onto Superfrost Gold slides. Sections were air dried for 48 hours and fixed in acetone prior to staining with haematoxylin and eosin or haematoxylin/van Gieson stains.

Cellular characterizations

Fluorescence immunocytochemistry (ICC)

At passages 0, 1 and 4, the cochlear and vestibular cell cultures were examined for the expression of the inner ear HC markers (myosin VIIa and prestin), SC markers (cytokeratin 18 and vimentin) and multipotent stem/progenitor cell markers (nestin and Sox2). Cells grown on 8-well chamber slides (Thermo Scientific Nunc; Lab Tek) were immunostained at confluence ≥80%. Initially, culture medium was removed and the cells were washed 3 times in DPBS, each wash was of 1 minute duration. The cells were then fixed by incubation in 4% paraformaldehyde for 15 minutes, followed by permeabilization in 0.1% Triton-X 100 for 15 minutes. Thereafter, the cells were blocked using 3% Bovine Serum Albumin (BSA) at room temperature for 30 minutes prior to incubation at 4^{o}C overnight with primary antibodies

[myosin VIIa (inner HC marker) 1:100 dilution (rabbit polyclonal- ab3481, ABCAM); prestin (outer HC marker) 1:100 dilution (goat polyclonal- SC22692, Santa Cruz Biotechnology); nestin (stem/progenitor cell marker) 1:100 dilution (rabbit polyclonal- ab92391, ABCAM); Sox2 (stem/progenitor cell marker) 1:100 dilution (rabbit polyclonal- ab97959 ABCAM); cytokeratin-18 (an epithelial cell marker) 1:50 dilution (mouse monoclonal - ab668, ABCAM) and vimentin (mesenchymal cell marker) 1:200 dilution (mouse monoclonal- ab20346, ABCAM and rabbit polyclonal- PA5-27231, Invitrogen)] dissolved in 3% BSA.

The following day, primary antibodies were drained and the chamber slides washed 3 times, each for 1 minute, in DPBS. Then, the cells were incubated at room temperature with secondary antibodies in the dark [goat anti-rabbit alexa fluor®488 1:500 dilution (ab150113, ABCAM); goat anti-mouse alexa fluor®488 1:500 dilution (ab150077, ABCAM); donkey anti-rabbit alexa fluor®488 1:500 dilution (A21206, Invitrogen); donkey anti-mouse alexa fluor®568 1:500 dilution (A10037, Invitrogen); and donkey anti-goat alexa fluor®488 1:500 dilution (A11055, Invitrogen)], respectively to the primary antibodies and shaken gently for 1 hour. The cells were then mounted with ProLong™ Gold Antifade Mountant with DAPI (P36931, Invitrogen). Images were captured using a Zeiss Axio Vert.A1 Inverted Microscope. HEI-OC1 cells served as the positive controls, and cells treated without primary antibody served as the negative controls.

Quantitative reverse transcription polymerase chain reaction (RT-qPCR) on adult porcine derived cochlear and vestibular cells

RNA was extracted from tissues and primary cell cultures of adult porcine derived cochlear and vestibular cells that were grown on T_{25} culture flasks. The level of mRNA expression of target genes *myosin VIIa*, *prestin*, *nestin*, *Sox2*, *cytokeratin 18* and *vimentin* was determined

212 at the tissue level and at passages 0, 2, 4 and 6 using the comparative Cycle threshold (ΔΔCt
213 method). A housekeeping gene for these experiments was selected by testing three candidate
214 genes *glyceraldehyde-3-phosphate dehydrogenase* (*Gapdh*), *beta-actin* (*b-Act*) and
215 *hypoxanthine phosphoribosyltransferase 1* (*Hprt1*) simultaneously. RefFinder, a web-based
216 tool was used to select the most stable of the candidate housekeeping genes tested by
217 computing the weighted geometric means of their individual rankings derived by four widely
218 used methods [17]. Target genes were also determined in positive control HEI-OC1 cells.
219
220 Primer3Plus software [18] was used to design the forward and reverse primers for both
221 porcine inner ear samples and HEI-OC1 cells (S1 Table and S2 Table, respectively). Primers
222 were designed for the genes associated with porcine inner ear HCs, SCs and stem/progenitor
223 cell characteristics using the GenBank (NCBI) database.
224
225 RNAs (RNeasy® mini kit, QIAGEN) were extracted from porcine cochlear and vestibular
226 tissues preserved in RNAlater held at -80^{o}C and from porcine (at P0, P2, P4 and P6) and
227 HEI-OC1 derived cell culture pellets which were dissolved in 350µl RLT buffer containing
228 0.01% 14.3M β-mercaptoethanol according to the manufacturer's instruction. The quantity
229 and quality of extracted RNAs were determined prior to cDNA preparation. We performed
230 cDNA synthesis with SuperScript™ VILO™ cDNA Synthesis Kit (Invitrogen) under the
231 following reaction conditions: 25^{o}C for 10 minutes, 42^{o}C for 60 minutes and 85^{o}C for 5
232 minutes (in a BioRadT100™ Thermal Cycler).
233
234 Synthesized cDNAs were then diluted to a concentration of 5ng/µl for RT-qPCR in a
235 StepOnePlus™ Instrument (Applied Biosystems) using 96-well plates and a SYBR Select
236 Master Mix reagent. In brief, the RT-qPCR reaction mix per well consisted of 1µl of

HyPure™ Molecular Biology Grade Water, 5µl SYBR Select Master Mix at the manufacturer's supplied concentration, 1µl of each forward and reverse primer (10µM) and 2µl of diluted cDNA (5ng/µl). After the reaction mix was added to the wells, the plate was centrifuged for few a seconds in a Mini PCR Plate Spinner. A RT-PCR consisted of an initial denaturing step of 95^{o}C for 10 minutes and followed by 40 amplification cycles of 15 seconds at 95^{o}C and 1minute at 60^{o}C for each cycle. Three replicates were taken from each sample.

Relative mRNA levels were determined using the comparative cycle threshold method at a cut off of Ct <35. The relative mRNA levels were expressed as the mRNA copies of the genes of interest per 1000 copies of *Hprt1* mRNA [$2^{-\Delta Ct}/1000 = 1000/2^{\Delta Ct} = 1000/2^{\wedge(\text{avg. target gene Ct} - \text{avg. housekeeping gene Ct})}$] [19, 20].

Statistical Analysis

The differences in the normalized mean Ct values of target genes between porcine cochlear and vestibular cells, and between porcine cochlear and HEI-OC1 cells were analyzed statistically using Student's *t*-test at a Benjamini-Hochberg corrected significance level of $p \leq 0.05$. The strength of correlation among different target gene expression levels within porcine cochlear and vestibular cell cultures was analyzed using a non-parametric Spearman's rank correlation coefficient test. Analyses were conducted using SPSS version 25.0 (IBM Corp., Armonk, New York). The level of statistical significance was set at $p < 0.01$.

Results

Adult porcine inner ear anatomy

Based on six temporal bone labyrinths selected at random from 12 adult pigs, the gross anatomy of the porcine labyrinth showed some similarity to human's. They both have a recognizable cochlear spiral though the pig's consisted of 3.5 turns compared to the human's 2.5 turns. There was a separate vestibular compartment arranged in raised bone canals. The six cochleas were found to have a mean maximal diameter and height of 7.99 and 3.77mm, respectively (Table 1). Average values ± standard error of mean are given. "A" denotes maximum axial diameter measured from the round window niche to the most lateral part of the basal turn of the cochlea. "B" denotes vertical axial diameter measured from helicotrema to the basal turn of the cochlea. "C" denotes short axis diameter measured between two opposite sides of the basal turn of the cochlea at right angles to measurement A. Measurements were taken using precision digital calipers to the nearest millimeter. Fig 1A illustrates how these measurements were made on a demineralised labyrinth.

Cochlea	A	B	C
1	7.97	3.72	7.38
2	8.01	3.66	7.31
3	8.03	3.70	7.32
4	7.97	3.95	7.40
5	7.96	3.76	7.36
6	7.98	3.85	7.37
Average ± standard error of mean	7.99 ± 0.01 mm	3.77 ± 0.04 mm	7.36 ± 0.01 mm

Table 1: Summary of gross measurements of six porcine inner ear specimens.

Fig 1. Adult porcine inner ear anatomy. A) A low power (10X) digital photomicrograph illustrates areas measured on a demineralized porcine inner ear that revealed a cochlea with

three and half turns. Measurements were made as follows (in mm): A- Maximum axial diameter-measured from round window niche to the most lateral part of basal turn of the cochlea; B- Vertical axial diameter-measured from helicotrema to basal turn of cochlea; C-Short axis diameter-measured between two opposite sides of the cochlea basal turn at right angles to A. **B)** A low power (10X) digital photomicrograph of a demineralized porcine inner ear showing the cochlea and the position of the cochlear implant electrode array. A cochlear implant electrode array has been inserted through a round window cochleaostomy to determine the cochlea length. The tip of the implant array can be seen at the helicotrema and the hub at the level of the round window. **C)** Photomicrograph of a haematoxylin and eosin stained mid-modiolar section through the *Sus scrofa* cochlea. Cross sectioning of the *S. scrofa* cochlea demonstrates compartments consistent with the scala tympani, media and vestibuli partitioned by the basilar and Reissner's membranes (indicated by arrows) identical to the arrangements found in the human cochlea.

Full insertion of a Nucleus C22 cochlear implant active electrode assembly through a round window cochleostomy was performed in two specimens such that the marker hub was level with the bony margin of the round window (Fig 1B). The tip of the electrode could be seen at the apex of the decalcified labyrinth in each case, leading to the conclusion that the pig's cochlear duct length is within 25.5-35.1 mm range. A Haematoxylin and Eosin stained cross-section shows the pig's bony cochlea to be partitioned into three compartments consistent with the scala tympani, media and vestibuli separated by the basilar and Reissner's membranes identical to the arrangements in human inner ear (Fig 1C). The cochlear duct contained abundant tissue for cell culture.

Cellular characterizations

Morphological characteristics of inner ear cells in in vitro culture

Porcine inner ear cells started to grow within 7-10 days of plating under *in vitro* conditions. Phase contrast microscopy illustrated that poricne inner ear derived cells at P0 contained a mixture of spindle shaped and flattened polyhedral shaped cells but by P4 there was a predominance of spindle shaped cells (Fig 2A to 2D). Proliferating cochlear tissue at P0 and P4 consisted of cell islands as shown in Fig 2A and 2B, respectively. Cells of similar appearance were seen in proliferating vestibular tissue at P0 and P4 (Fig 2C and 2D, respectively). Primary cell cultures consisted of heterogenous cells and formed monolayers which showed a high level of adhesion onto plastic surfaces. HEI-OC1 cells predominantly consisted of spindle shaped cells (Fig 2E) similar to P4 and later porcine derived inner ear cultured cells.

Fig 2. Morphology of inner ear *in vitro* cell cultures demonstrated by phase contrast microscopy. A) and **C)** Proliferating cochlear and vestibular cultures at passage 0; **B)** and **D)** Cochlear and vestibular cell cultures consisted of cell islands at passage 4 (indicated by white arrows); **E)** Positive control HEI-OC1 cells. The magnifications are given in each panel.

Porcine inner ear cells and HEI-OC1 cells grown on coated 8-well chamber slides showed similar sphere-forming charactericitics *in vitro* using phase-contrast microscopy (Fig 3A). SEM revealed that the sphere-forming HEI-OC1 (Fig 3B) porcine cochlear (Fig 3C and porcine vestibular cells (Fig 3D) were oblong in shape with large and small cytoplasmic protrusions on their surfaces.

Fig 3. Sphere-forming characteristics of inner ear cells in *in vitro* cultures. A) Phase contrast microscopy demonstrated sphere-forming characteristics of porcine inner ear cells

and HEI-OC1 cells grown on coated 8-well chamber slides. **B)** SEM revealed sphere-forming cells within the HEI-OC1 cultures that demonstrated prominent surface protrutions and cytoplasmic projections. **C)** Sphere-forming cells in porcine cochlear cultures similarly bore considerable protrusions on their surfaces and cytoplasmic projections. **D)** Sphere-forming cells in porcine vestibular cultures were similar though with less protrusions on their surfaces. Passaged 4 porcine inner ear *in vitro* cultures were used for SEM study.

Higher resolution SEM images of porcine derived inner ear cells revealed sphereical structures arising from cells with ciliary-type surface projections (Fig 4) *in vitro*. Cells with ciliary-type projections in HEI-OC1 culture (Fig 4A) and in porcine cochlear culture at P4 (Fig 4B) showed disorganized stereocilia-like structures with appendages suggestive of broken inter-stereociliary links (indicated by black arrows). Sphere-forming cells in the porcine vestibular cultures at P4 bore microvillar-like projections that varied in length some long and others short (Fig 4C).

Fig 4. SEM characteristics of cells bearing ciliary-type projections on their surfaces. A) and **B)** Higher resolution SEM of sphere-forming cells with disorganized stereocilia-like structures with broken inter-stereociliary links (indicated by black arrows) in HEI-OC1 and porcine cochlear cells, respectively. **C)** Porcine vestibular cells are similarly shown to possess microvillar-like projections on their surfaces that vary in length though lacking any directional arrangement into rows of increasing length. Passage 4 porcine inner ear *in vitro* cultures were used for SEM study. Image resolution is indicated in each panel in micrometers.

Fluorescence immunocytochemistry

Stem/progenitor cell markers nestin and Sox2 were identified in adult derived porcine inner ear *in vitro* cultures (Fig 5). Nestin positive cells were plentiful in both cochlear (Fig 5A) and vestibular (Fig 5G) cell cultures at P1 and P4, respectively. Sox2 was localized in the nuclei of few porcine cochlear (Fig 5C) and vestibular (Fig 5H) cells at P1 and P4, respectively. More cells in both cochlear and vestibular cultures were positive for nestin rather than for Sox2 across the passages. Cell islands found in porcine vestibular cultures elicited strong signals to both nestin and Sox2 markers (indicated by white arrows). HEI-OC1 cells demonstrated a similar nestin (Fig 5B) and Sox2 (Fig 5D) expression pattern to porcine cochlear cells. Additionally, some of the globular or spherical shaped cells in porcine inner ear and HEI-OC1 cell cultures expressed both nestin and Sox2 (indicated by yellow arrows) markers. SEM demonstrated possible corresponding globular or spherical shaped cells with protrusions and long villi on their surface in porcine cochlear and HEI-OC1 cell cultures as shown in Fig 5E and 5F, respectively. These types of cells were observed consistently across all passages.

Fig 5. Presence of multipotent stem/progenitor cells in *in vitro* cultures. A) and **G)** Nestin positive cells were identified in the cochlear and vestibular cells at passages 1 and 4, respectively. **C)** and **H)** Sox2 positive nuclei were detected in the cochlear and vestibular cells at passages 1 and 4, respectively. **B)** Nestin positive cells in HEI-OC1 cells; **D)** Sox2 positive nuclei within the HEI-OC1 cells; **E)** and **F)** SEM images of a globular or spherical shaped cell with protrusions and long villi on its surface identified within the porcine cochlear and HEI-OC1 cell cutures, respectively. White arrows indicate the cell islands positive to both nestin and Sox2 markers within vestibular cultures at passage 4. DAPI was used to stain the nuclei (blue). Phase contrast microscopic images are given at magnification 400X. SEM image resolution is indicated in each panel in micrometers.

HC markers myosin VIIa and prestin positive cells were identified in porcine derived inner ear cell cultures based on immunofluorescence staining, although the intensity and dispersion varied across the cell passages (Fig 6).

Fig 6. Localization of hair cell markers prestin and myosin VIIa. A) and **D)** Prestin localization identified in proliferating cochlear and vestibular tissues, respectively at passage 0 (indicated by yellow arrows). **B)** and **E)** Prestin plasma membrane localization strongly detected in cochlear and vestibular cells at passage 4 (indicated by yellow arrows). **C)** Prestin expression identified in HEI-OC1 cells. **F)** and **G)** Myosin VIIa expressions at passages 0 and 4 identified in cochlear cell cultures. **I)** and **J)** Myosin VIIa expressions at passages 0 and 4 identified in vestibular cell cultures. **G)** Myosin VIIa expression identified in HEI-OC1 cells. DAPI was used to stain the nuclei (blue). Phase contrast microscopic images are given at magnification 400X.

Prestin was localized in proliferating tissues of both the cochlea (Fig 6A) and vestibule (Fig 6D) at P0 and the expression was visibly stronger in cochlear than in vestibular *in vitro* cultures (indicated by yellow arrows). At P4, prestin expression was localized to the plasma membrane of cochlear (Fig 6B) and vestibular cells (Fig 6E) as indicated by yellow arrows. Prestin expression in HEI-OC1 cells was similarly localized as shown in Fig 6C. Prestin expression levels in both adult porcine derived cochlear and vestibular cells were visibly stronger than that of the positive control HEI-OC1 cells.

Myosin VIIa expression was strong and localized within the cytoplasm in adult porcine derived cochlear (Fig 6F and 6G) and vestibular (Fig 6I and 6J) cultured cells and in HEI-

405 OC1 cells (Fig 6H). In contrast to the prestin marker, at P0, myosin VIIa expression was
406 widely distributed throughout the porcine cochlear and vestibular derived *in vitro* cultured
407 cells in keeping with diffuse cytoplasmic apical projections (Fig 6F and 6I, respectively). At
408 P4, the myosin VIIa expression levels in porcine cochlear and vestibular cells (Fig 6G and 6J,
409 respectively) were visibly stronger than in HEI-OC1 cells (Fig 6H) or P0 porcine derived
410 cells. At P4, myosin VIIa positive signals were densely packed in both the porcine cochlear
411 and vestibular cells compared to P0 cells.
412
413 At P0, SC protein markers, particularly cytokeratin 18 was vigorously expressed compared to
414 vimentin in both cochlear (Fig 7A and 7B) and vestibular (Fig 7B and 7D) cultures,
415 respectively. Cytokerain 18 expressing cells were compartively larger in size and polyhedral
416 in shape. Vimentin expressing cells were comparatively smaller in size and mostly spindle
417 shaped. At P4, vimentin was comparatively strongly expressed in cochlear and vestibular
418 cells (Fig 7E and 7F, respectively), in contrast, cytokeratin 18 was weakly expressed in both
419 cochlear and vestibular cells (Fig 7G and 7H, respectively). Vimentin and cytokeratin 18
420 protein experssions were comparable to each other in HEI-OC1 cells (Fig 7I and 7J,
421 respectively) and they were smaller in size than porcine cells and mostly spindle shaped.
422
423 **Fig 7. Immunolocalization of supporting cell markers vimentin and cytokeratin 18.**
424 Expression for: **A)** and **B)** vimentin at passage 0 in cochlear and vestibular cultures,
425 respectively; **C)** and **D)** cytokeratin 18 at passage 0 in cochlear and vestibular cultures,
426 respectively; **E)** and **F)** vimentin at passage 4 in cochlear and vestibular cultures,
427 respectively; **G)** and **H)** cytokeratin 18 at passage 4 in cochlear and vestibular cultures,
428 respectively; **I)** and **J)** vimentin and cytokeratin 18 positive HEI-OC1 cells, respectively.

DAPI was used to stain the nuclei (blue). Phase contrast microscopic images are given at magnification 400X.

Double antibody labelling for myosin VIIa and cytokeratin 18 elicited strong signals within the porcine inner ear and HEI-OC1 cell cultures (Fig 8). Porcine vestibular cultures contained double-labelled epithelial cell islands (Fig 8A) at P4. Similarly, porcine cochlear culture showed double-labelled cells (Fig 8B) at P4, and the expression patterns were comparable to HEI-OC1 cells (Fig 8C).

Fig 8: Double-labelled immunofluorescence demonstrated the co-localization of inner ear HC and SC markers. A) and **B)** Porcine vestibular and cochlear cells demonstrated dual labelling for antibodies cytokeratin 18 (green) and myosin VIIa (red) at passage 4; **C)** Double-labelled cells for cytokeratin 18 and myosin VIIa markers in HEI-OC1 cells. Closely packed myosin VIIa positive apical projections around the nucleus are indicted by yellow arrows. DAPI was used to stain the nuclei (blue). Phase contrast microscopic images are given at magnification 400X.

Relative gene expressions

In this study, three housekeeping genes, *b-actin*, *Hprt1* and *Gapdh*, were tested to determine RNA expression stability for RT-qPCR data normalization in cochlear and vestibular cell cultures throughout the passages. In cochlear cell cultures, from harvested tissues to P6, mean Ct value ± standard deviation (S.D.) for *Hprt1* was 23.41 ± 1.01, *Gapdh* was 16.59 ± 1.63, and *b-Act* was 14.38 ± 2.18. In vestibular cell cultures, from harvested tissues to P6, mean Ct value ± S.D. for *Hprt1* was 22.4 ± 1.01, *Gapdh* was 15.71 ± 1.58, and *b-Act* was 13.76 ± 2.52. *Hprt1* mRNA expression was most stable across the passages, compared to *Gapdh* and

454 *b-Act*. RefFinder software ranked the prospective housekeeping genes in order of the most to
455 the least stable *as Hprt1, Gapdh and b-actin*.
456
457 The relative mRNA levels of these genes in harvested cochlea and vestibule membranous
458 tissues are illustrated (Fig 9A). The targeted genes normalized mean Ct values when
459 compared between cochlear and vestibular harvested tissues, demonstrated that m*yosin VIIa*
460 expression levels in cochlear and vestibular tissues were almost identical ($p = 0.947$),
461 whereas *prestin* expression was greater in cochlear tissue with a statistical significance at $p =$
462 0.029. Gene *Sox2* ($p = 0.036$) was significantly highly expressed in vestibular tissue whereas
463 genes *nestin* ($p = 0.113$), *cytokeratin 18* ($p = 0.12$) and *vimentin* ($p = 0.059$) were not
464 significantly different between porcine cochlear and vestibular harvested tissues.
465
466 **Fig 9. Relative gene expressions within cochlear (blue) and vestibular (orange) *in vitro***
467 **cell cultures**. **A)** Relative mRNA levels of *myosin VIIa, prestin, nestin, Sox2, cytokeratin 18*
468 and *vimentin* are presented for harvested adult porcine cochlea and vestibule in log base 2. **B)**
469 to **G)** Relative mRNA levels of *myosin VIIa, prestin, nestin, Sox2, cytokeratin 18* and
470 *vimentin* in *in vitro* cultures. Gene *hypoxanthine phosphoribosyltransferase 1* (*Hprt1*) was
471 used as an endogeneous control. Positive control was HEI-OC1 cells (indicated by black).
472 Number of replicates were three and the error bars represented the standard error.
473
474 The target genes' normalized mean Ct values varied between porcine cochlear and vestibular
475 cells. m*yosin VIIa* expression was significantly highly expressed at P4 ($p = 0.000006$) in
476 cochlear compared with vestibular cells (Fig 9B). Similarly, *prestin* expression was
477 significantly highly expressed at P4 ($p = 0.00003$) and at P6 ($p = 0.024$) in cochlear compared
478 with vestibular cells (Fig 9C). Genes *Sox2* (Fig 9E) and *cytokeratin 18* (Fig 9F) were

479 significantly highly expressed in cochlear cells at all tested passages: P0 ($p = 0.017$, $p = 0.04$), P2 ($p = 0.001$, $p = 0.011$), P4 ($p = 0.00005$, $p = 0.00004$) and P6 ($p = 0.0001$, $p = 0.0002$), respectively. *Nestin* at P2 ($p = 0.015$) and P4 ($p = 0.01$) (Fig 9D) and *vimentin* at P0 ($p = 0.008$) and P4 ($p = 0.005$) (Fig 9G) were also significantly highly expressed in cochlear compared with vestibular cells.

484

485 The normalized mean Ct values of all tested genes in porcine cochlear cells were significantly
486 different ($p < 0.05$) across the passages 0 to 6 when compared with HEI-OC1 cells except for
487 *nestin* expression at P6 ($p = 0.26$) and *vimentin* expression at P0 ($p = 0.42$) (Fig 9D and 9G,
488 respectively). *Prestin* gene expression was undetectable in HEI-OC1 cells, thus statistical
489 analysis was not performed.

490

491 The level of expression of of *cytokeratin 18*, and both HC markers *myosin VIIa* and *prestin*
492 were significantly positively correlated [$p = 0.005$, Spearman correlation (τ) = 0.943] in
493 porcine cochlear cultures, from harvested tissue to P6. Genes *myosin VIIa* and *prestin*
494 expressions demonstrated a signifcant positive correlation in both porcine cochlear ($p =$
495 0.019, $\tau = 0.886$) and vestibular ($p = 0.005$, $\tau = 0.943$) cultures, from harvested tissue to P6.
496 Porcine vestibular cultures also demonstrated a significant positive correlation between *nestin*
497 and *prestin* mRNA levels from harvested tissue to P6 ($p = 0.019$, $\tau = 0.886$).

498

499 ## Discussion

500 We demonstrated that the pig's labyrinth was anatomically similar to that of the human's
501 which is consistent with other studies [21, 22]. The maximal transverse and vertical axial
502 diameters of the pig's cochleas sampled are consistent with the findings reported in a large
503 series of human cochleas [23]. Our use of an inserted cochlear implant electrode ascertained

the length of the pig's cochlea duct as 35mm in two specimens which is within the range of lengths of the human cochleas based on anatomical studies [24] and the mean lengths derived from CT data [25]; 28.0-40.1 mm and 34.62 mm, respectively. These findings indicate that the pig's cochlear dimensions (length and cross sectional diameter) are similar to those of the human cochlea.

The development, function, and maintenance of inner ear sensory epithelia are heavily dependent upon the SCs [26], which are crucial in cochlea homeostasis. Hence, our aim was to develop an *in vitro* multi-cellular culture which mirrors the complexity of the human inner ear to facilitate the use of these cells in studies of hearing and balance disorders. Our findings indicate that primary cell cultures of adult porcine derived inner ear cochlear and vestibular cells are heterogeneous, highly adherent to plastic surfaces and demonstrate the presence of inner ear HC, SC and multipotent stem/progenitor cell characteristics based on SEM, fluorescence immunocytochemistry and RT-qPCR.

Sphere-forming cells were observed in both porcine cochlear and vestibular cell cultures and were similar to those observed in HEI-OC1 cultures. This suggests that these cultures contain cells with or that develop stem-like properties in the culture conditions we utilised. It remains unclear whether mammalian inner ear sphere-forming cells are endogenous stem cells or derived from SCs. In non-mammalian vertebrates such as birds, fish and amphibians, SCs are the most likely source of progenitor cells within the inner ear sensory epithelia [9]. These SCs can generate new HCs either via a regenerative response of dedifferentiation, proliferation and differentiation, or a direct phenotype conversion called trans-differentiation [9, 27]. It has been reported that vestibular sensory epithelia SCs display stem cell characteristics in mature guinea pigs and in adult humans *in vitro* [2, 3]. In mice, adult

529 vestibular SCs replace damaged HCs to a certain extent [28], in contrast, cochlear SCs lose
530 this capacity during the first few neonatal weeks as the inner ear completes its maturation
531 [28-30]. Recent demonstrations of spontaneous HC regeneration in the immature neonatal
532 mouse cochlea suggest that progenitor cells in that species are generated primarily by trans-
533 differentiation of SCs and not by the proliferation of existing stem cells or dedifferentiation
534 of SCs into stem cells [31, 32]. Although SCs with the capability for phenotypic conversion
535 to HCs have been identified, such capability within the organ of Corti is only demonstrated in
536 prenatal and neonatal rodent models where HCs and SCs are still developing [33-35]. Since
537 the early postnatal cochlea of the mouse is immature, the relevance of these findings to
538 regenerative therapies in adult humans is unclear [36].
539
540 In most previous studies, inner ear multipotent cells were induced to differentiate into cells
541 expressing HC markers in part by adhesion to substrates, such as poly-D-lysine [37], poly-L-
542 lysine [38, 28], fibronectin [39] and laminin [40]. Liu et al. [38] promoted differentiation of
543 inner ear multipotent cells derived from postnatal day 0 mice cochlear sensory epithelia into
544 functional HC-like cells containing characteristic stereocilia bundles through a two-step-
545 induction method. Ding et al. [40] described similar techniques that induced the conversion
546 of human embryonic stem cells into otic epithelial progenitors (OEPs) followed by the
547 induced differentiation of OEPs into HC-like cells not only by substrate selection but also the
548 deployment of conditioned media containing epidermal growth factor and all-trans retinoic
549 acid. We did not use any growth factor media beyond DMEM plus 10% FBS and obtained
550 HC-like cells from adult porcine inner ear cells which were similar on SEM to the HC-like
551 cells obtained by Liu et al. [38] and Ding et al. [40]. Ding et al. [40] however demonstrated
552 that HC-like cells that were induced on a substrate of mitotically inactivated chicken utricle
553 stromal cells were functional and displayed more organized surface ciliary architecture than

554 those that were induced on a poly-L-lysine substratum. They hypothesized that stromal
555 substrate cells may release factors that are important for the development of functional HCs.
556 Although, the HC-like cells that we generated displayed similar SEM characteristics, further
557 work is required to determine their functional status. Importantly, we utilized the multiple
558 cell types present in the inner ear as the starting point for our experiments thus we submit that
559 any necessary factors that Ding et al. [40] hypothesized to be present in their utricle stomal
560 cell substrate may be present in our *in vitro* cultures. Nonetheless these observations
561 demonstrate a more direct method of generating HC-like cells from postmortem adult porcine
562 labyrinth specimens than previously described techniques.
563
564 Immunofluorescence staining and RT-qPCR revealed that nestin was strongly expressed in
565 both porcine cochlear and vestibular cultures across the passages 0 to 6 comparable to that
566 seen in HEI-OC1 cell cultures. Nestin-positive cells have been found in tissue or organ-
567 specific sites, where they serve as quiescent cells capable of proliferation, differentiation, and
568 migration after their reactivation [41]. Nestin is associated with pluripotency in embryonic
569 and induced pluripotent stem cells, as well as multipotency in spiral ganglion cells of the
570 mature mouse [42]. Several studies have shown that nestin-positive cells derived from inner
571 ear cells or embryonic stem cells serve as progenitors for sensory HC-like cells [43-45].
572 Chow et al. [42] found nestin-expressing cells adjacent to the inner HC layer in postnatal and
573 young adult mice. Nestin-positive cells in the mature rat cochlea have been identified as SCs
574 situated laterally, adjacent to outer HCs in the cochlea apex [46]. Lou et al.'s [47] study on
575 cultivated cochlear cells derived from adult and neonatal mice suggests that stem/progenitor
576 cells maintained their stemness but eventually lose the potential to differentiate into other cell
577 types with age. Therefore, we propose that the strong nestin-expressing cells in porcine inner
578 ear and HEI-OC1 cell cultures are multi- or oligo-potent progenitors that generate HC and

579 SC-like inner ear cells especially when grown on poly-L-lysine coated surfaces. However,
580 more work is required to identify the location and specific cell type(s) which demonstrate
581 stem/progenitor cell activity within the porcine inner ear.
582
583 Mammalian stereocilia contain myosin VIIa which maintains the structural integrity of the
584 HC bundles [48, 49]. HC-like cells with disorganized stereocilia were identified by SEM in
585 the passaged porcine *in vitro* cultures. We also undertook SEM on cultured HEI-OC1 cells
586 which to our knowledge has not been previoulsy reported and found HC-like with
587 disorganized sterocilia similar to those in the porcine cultures. Although, myosin VIIa
588 positive cells were identified using ICC in both porcine cochlear and vestibular cells from
589 passages 0 through 6, relative *myosin VIIa* mRNA expression was identified at lower levels
590 in passaged cultures than expected based on the ICC and SEM findings. The high number of
591 HC-like cells on SEM and ICC may be due to the poly-L-lysine coating on the slides and
592 coverslips used for these experiments as this substrate has been previously demonstrated to
593 induce the conversion of multipotent stem/progenitor cells into HC-like cells [38, 40].
594 Similarly as the cell culture flasks used for qPCR were not coated with poly-L-lysine the
595 same degree of induction of HC-like cells will not have occurred. Alternatively the
596 differences in myosin VIIa cellular protein distribution and mRNA concentration may be a
597 reflection of differences in the degree to which the cultured HC-like cells have differentiated
598 to resemble functional HCs.
599
600 The co-localization of myosin VIIa and cytokeratin 18 in porcine cochlear and vestibular
601 cells is consistent with that expected in immature HCs as cytokeratin is abundant in HC
602 progenitor cells after which the level decreases progressively as HCs mature until it is no
603 longer present in mature HCs [50]. The significant positive correleation between c*ytokeratin*

18 and *myosin VIIa* mRNA expressions within the porcine cochlear cultures further supports the presence of immature HC-like cells across the passages.

The outer HC marker prestin belongs to the mammalian SLC26 family [51]. Recently, Park et al. [52] studied the HEI-OC1 auditory cells as a model for investigating prestin function. They confirm that under permissive conditions (33^{o}C, 10% CO_2), a condition in which HEI-OC1 cells proliferate *in vitro*, prestin is expressed mostly in the cytoplasm; in contrast, under non-permissive conditions (39^{o}C, 5% CO_2), a condition in which HEI-OC1 cells differentiate *in vitro*, total prestin expression is increased and localized to the plasma membrane. Our cell culture conditions (37^{o}C, 5% CO_2) are close to non-permissive conditions and we observed strong prestin expression in the plasma membranes of both adult porcine inner ear cells and HEI-OC1 cells *in vitro*. Similar to Adler et al. [53], we identified prestin protein in vestibular cell cultures; although prestin is primarily designated as an outer HC motor protein of the mammalian cochlea. The relative *prestin* mRNA level decreased from harvested tissues through P6 cell cultures and was undetectable in HEI-OC1 cells; however, plasma membrane prestin protein localization persisted across the passages when grown on coated 8-well chamber slides. These findings provide further evidence that the HC-like cells observed on SEM analysis of the porcine cell cultures grown on coated slides or cover slips possess differentiated HC-like characteristics.

The adult porcine derived inner ear cell *in vitro* cultures displayed a higher level of vimentin mRNA than the level in the harvested tissues. This may be a reflection of a high level of proliferation in the cultured cells as *vimentin* is associated with mitosis and cell growth [54]. Vimentin is present in several inner ear cell types which means that it lacks specificity as a marker of a single cell type. The cytoplasm of mammalian inner ear SCs including Deiters

629 and inner pillar cells are vimentin rich [55] and in addition contain cytokeratin. Spiral
630 ligament fibrocytes amongst others are a rich source of fibroblasts. In addition, the culture
631 media contained FBS supplement a promoter of fibrobastic proliferation. Therefore the
632 combination of a number of *vimentin* expressing cell types all of which are rapidly dividing
633 may account for the increased *vimentin* mRNA levels in the cultured cells compared to the
634 harvested tissues.
635
636 To our knowledge, housekeeping genes for RT-qPCR studies on porcine derived inner ear
637 cells have not been previously published. We identified *Hprt1* as a suitable housekeeping
638 gene for investigating genes in porcine inner ear tissue by comparison with *Gapdh* and *b-Act*
639 which is consistent with Nygard et al.'s findings in other porcine tissues [56].
640

641 ## Conclusion

642 Taken together, the similarity of the pig's inner ear anatomy and cellular composition to that
643 of humans suggest that the domestic pig can be considered as an animal model for the study
644 of human inner ear disorders. Our findings suggest that adult porcine cochlea and vestibule
645 tissue have the capacity to form new HC populations. Furthermore, we found evidence for
646 multipotent stem/progenitor cells in adult derived inner ear *in vitro* cultures though additional
647 work is required to identify the cell type(s) and the location of these cells within the porcine
648 inner ear.
649

650 **Conflicts of Interest**

651 The authors have declared that no competing interests exist.
652

653 **Acknowledgements**

The authors thank Dr. F. Kalinec, Laboratory Auditory Cell Biology, Dept. of Head & Neck Surgery, David Geffen Scholl of Medicine at UCLA, Los Angeles, CA, USA for gifting HEI-OC1 cells. Our sincere thanks to Mr. Derrick Horne, Technical Specialist, UBC Bioimaging Facility, Vancouver Campus for his technical assistance to carry out the scanning electron microscopy on passaged in inner ear cell *in vitro* cultures.

Funding Statement

We acknowledge the funding agencies: North Bristol NHS Trust Small Grant Scheme RD47, Bristol, United Kingdom; North Bristol NHS Trust Department of Otolaryngology Postgraduate Study Grant, Bristol, United Kingdom; Vancouver Coastal Health Research Institute 20R22867, Vancouver, Canada; Rotary Hearing Foundation, Vancouver, Canada; and Pacific Otolaryngology Foundation, Vancouver, Canada for their financial support.

Author contributions

D.A.N. proposed the study and obtained funding. D.A.N., A.S., T.A.C. and P.W. designed the experiments and interpreted the results. P.W. and A.S. drafted the paper. D.A.N. and E.H. revised the paper. A.S., T.A.C., P.W., B.Z., E.H., G.H. and J.K. developed the cell cultures. P.W. performed the cellular characterization studies. P.W. analysed the data. A.S. and T.A.C. performed the anatomical studies. All authors reviewed the final manuscript.

References

1) Muller U, Barr-Gillespie PG. New treatment options for hearing loss. Nat Rev Drug Discov. 2015 Mar 20;14(5):346-65. PMID: 25792261.

2) Forge A, Li L, Nevill G. Hair cell recovery in the vestibular sensory epithelia of mature guinea pigs. J Comp Neurol. 1998 Jul 20; 397(1):69-88. PMID: 9671280.

679 3) Warchol ME, Lambert PR, Goldstein BJ, Forge A, Corwin JT. Regenerative proliferation
680 in inner ear sensory epithelia from adult guinea pigs and humans. Science. 1993 Mar 12;
681 259(5101):1619-22. PMID: 8456285.
682 4) Taylor RR, Jagger DJ, Saeed SR, Axon P, Donnelly N, Tysome J, et al. Characterizing
683 human vestibular sensory epithelia for experimental studies: new hair bundles on old tissue
684 and implications for therapeutic interventions in ageing. Neurobiol Aging. 2015
685 Jun;36(6):2068-84. PMID: 25818177.
686 5) Golden EJ, Benito-Gonzalez A, Doetzlhofer A. The RNA-binding protein LIN28B
687 regulates developmental timing in the mammalian cochlea. Proc Natl Acad Sci USA. 2015
688 Jul 2;112(29):E3864-73. PMID: 26139524.
689 6) Lin V, Golub JS, Nguyen TB, Hume CR., Oesterle EC, Stone JS. Inhibition of Notch
690 activity promotes nonmitotic regeneration of hair cells in the adult mouse utricles. J Neurosci.
691 2011 Oct 26;31(43):15329–39. PMID: 22031879.
692 7) Li L, Forge A. Morphological evidence for supporting cell to hair cell conversion in the
693 mammalian utricular macula. Int J Dev Neurosci. 1997 Jul;15(4-5):433–46. PMID: 9263024 .
694 8) Corwin JT, Oberholtzer JC. Fish n' chicks: model recipes for hair cell regeneration?
695 Neuron. 1997 Nov;19(5):951-4. PMID: 9390508.
696 9) Rubel EW, Furrer SA, Stone JS. A brief history of hair cell regeneration research and
697 speculations on the future. Hear Res. 2013 Mar;297:42-51. PMID: 23321648.
698 10) Savary E, Hugnot JP, Chassigneux Y, Travo C, Duperray C, Van De Water T, et al.
699 Distinct population of hair cell progenitors can be isolated from the postnatal mouse cochlea
700 using side population analysis. Stem Cells. 2007 Feb;25(2):332–9. PMID: 17038670.
701 11) Humphray SJ, Scott CE, Clark R, Marron B, Bender C, Camm N, et al. A high utility
702 integrated map of the pig genome. Genome Biol. 2007 Jul 11;8(7):R139. PMID: 17625002.

12) Gutierrez K, Dicks N, Glanzner WG, Agellon LB, Bordignon V. Efficacy of the porcine species in biomedical research. Front Genet. 2015 Sep 16;(6):293. PMID: 26442109.

13) Groenen MA, Archibald AL, Uenishi H, et al. Analyses of pig genomes provide insight into porcine demography and evolution. Nature. 2012 Nov 15;491(7424):393-8. PMID: 23151582.

14) Guo W, Yi H, Ren L, Chen L, Zhao L, Sun W, et al. The morphology and electrophysiology of the cochlea of the miniature pig. Anat Rec. 2015 Mar;298(3):494-500. PMID: 25394601.

15) Kalinec GM, Park C, Thein P, Kalinec F. Working with auditory HEI-OC1 cells. J Vis Exp. 2016 Sep 3;115:54425. PMID: 27684094.

16) Li Y, Jia S, Liu H, Tateya T, Guo W, Yang S, et al. Characterization of hair cell-like cells converted from supporting cells after notch inhibition in cultures of the organ of Corti from Neonatal Gerbils. Front Cell Neurosci. 2018 Mar 20;12:73. PMID: 29662441.

17) Xie F, Xiao P, Chen D, Xu L, Zhang B. miRDeepFinder: a miRNA analysis tool for deep sequencing of plant small RNAs. Plant Mol Biol. 2012 Jan 31;80:75-84. PMID: 22290409.

18) Untergasser A, Nijveen H, Rao X, Bisseling T, Geurts R, Leunissen JA. Primer3Plus, an enhanced web interface to Primer3. Nucleic Acids Res. 2007 Jul;35:W71-4. PMID: 17485472.

19) Huang Y, Litvinov IV, Wang Y, Su MW, Tu P, Jiang X, et al. Thymocyte selection-associated high mobility group box gene (TOX) is aberrantly over-expressed in mycosis fungoides and correlates with poor prognosis. Oncotarget. 2014 Jun 30;5:4418-25. PMID: 24947046.

20) Schmittgen TD, Livak KJ. Analyzing real-time PCR data by the comparative C(T) method. Nat Protoc. 2008 Jun 5;3(6):1101-8. PMID: 18546601.

21) Yi H, Guo W, Chen W, Chen L, Ye J, Yang S. Miniature pigs: a large animal model of cochlear implantation. Am J Transl Res. 2016 Dec 15;8(12):5494-502. PMID: 28078020.

22) Gurr A, Kevenhorster K, Stark T, Pearson M, Dazert S. The common pig: a possible model for teaching ear surgery. Eur Arch Oto-rhino-laryngol. 2010 Jul 12;267(2):213-7. PMID: 19597737.

23) Dimopoulos P, Muren C. Anatomic variations of the cochlea and relations to other temporal bone structures. Acta Radiol. 1990 Sep;31(5):439-44. PMID: 2261286.

24) Ulehlová L, Voldrich L, Janisch R. Correlative study of sensory cell density and cochlear length in humans. Hear Res. 1987;28(2-3):149-51. PMID: 3654386.

25) Skinner MW, Ketten DR, Holden LK, Harding GW, Smith PG, Gates GA, et al. CT-derived estimation of cochlear morphology and electrode array position in relation to word recognition in Nucleus-22 recipients. J Assoc Res Otolaryngol. 2002 Sep 3;3(3):332-50. PMID: 12382107.

26) Wan G, Corfas G, Stone, J S. Inner ear supporting cells: Rethinking the silent majority. Semin Cell Dev Biol. 2013 May;24(5):448-59. PMID: 23545368.

27) Adler HJ, Raphael Y. New hair cells arise from supporting cell conversion in the acoustically damaged chick inner ear. Neurosci Lett. 1996 Feb 16;205(1):17-20. PMID: 8867010.

28) Oshima K, Grimm CM, Corrales CE, Senn P, Monedero RM, Géléoc GSG, et al. Differential distribution of stem cells in theauditory and vestibular organs of the inner ear. J Assoc Res Otolaryngol. 2007 Mar;8(1):18–31. PMID: 17171473.

29) Doetzlhofer A, White P, Lee YS, Groves A, Segil N. Prospective identification and purification of hair cell and supporting cell progenitors from the embryonic cochlea. Brain Res. 2006 May 26;1091(1):282-8. PMID: 16616734.

751 30) White PM, Doetzlhofer A, Lee YS, Groves A, Segil N. Mammalian cochlear supporting
752 cells can divide and trans-differentiate into hair cells. Nature. 2006 Jun 22;441(7096):984-7.
753 PMID: 16791196.
754 31) Bramhall NF, Shi F, Arnold K, Hochedlinger K, Edge AS. Lgr5-positive supporting cells
755 generate new hair cells in the postnatal cochlea. Stem Cell Rep. 2014 Mar 11;2(3):311-22.
756 PMID: 24672754.
757 32) Cox BC, Chai R, Lenoir A, Liu Z, Zhang L, Nguyen DH, et al. Spontaneous hair
758 regenerations in the neonatal mouse cochlea in vivo. Development. 2014 Feb;141(4):816-29.
759 PMID: 24496619.
760 33) Xu J, Ueno H, Xu CY, Chen B, Weissman IL, Xu PX. Identification of mouse cochlear
761 progenitors that develop hair and supporting cells in the organ of Corti. Nat Commun. 2017
762 May 11;8:15046. PMID: 28492243.
763 34) Gubbels SP, Woessner DW, Mitchell JC, Ricci AJ, Brigande JV. Functional auditory hair
764 cells produced in the mammalian cochlea by in utero gene transfer. Nature. 2008 Sep
765 25;455(7212):537-41. PMID: 18754012.
766 35) Zheng JL, Gao WQ. Overexpression of Math 1 induces robust production of extra hair
767 cells in postnatal rat inner ears. Nat Neurosci. 2000 Jun;3(6):580-6. PMID: 10816314.
768 36) Takeda H, Dondzillo A, Randall JA, Gubbels SP. Challenges in cell-based therapies for
769 the treatment of hearing loss. Trends Neurosci. 2018 Nov;41(11):823-37. PMID: 30033182.
770 37) Diensthuber M, Oshima K, Heller S. Stem/progenitor cells derived from the cochlear
771 sensory epithelium give rise to spheres with distinct morphologies and features. J Assoc Res
772 Otolaryngol. 2009 Jun;10(2):173-90. PMID: 19247714.
773 38) Liu Q, Shen Y, Chen J, Ding J, Tang Z, Zhang C, et al. Induction of functional hair-cell-
774 like cells from mouse cochlear multipotent cells. Stem Cells Int. 2016 Dec 29;2016:8197279.
775 PMID: 27057177.

776 39) Savary E, Sabourin JC, Santo J, Hugnot JP, Chabbert C, Van de Water T, et al. Cochlear
777 stem/progenitor cells from a postnatal cochlea respond to Jagged1 and demonstrate that notch
778 signaling promotes sphere formation and sensory potential. Mech Dev. 2008
779 Aug;125(8):674–86. PMID: 18571907.
780 40) Ding J, Tang Z, Chen J, Shi H, Chen J, Wang C, et al. Induction of differentiation of
781 human embryonic stem cells into functional hair-cell-like cells in the absence of stromal
782 cells. Int J Biochem Cell Biol. 2016 Dec;81(Pt A):208-22. PMID: 26615761.
783 41) Wiese C, Rolletschek A, Kania G, Blyszczuk P, Tarasov KV, Tarasova Y, et al. Nestin
784 expression—a property of multi-lineage progenitor cells? Cell Mol Life Sci. 2004 Oct;61(19-
785 20):2510-22. PMID: 15526158.
786 42) Chow C L, Trivedi P, Pyle MP, Matulle JT, Fettiplace R, Gubbels SP. Evaluation of
787 nestin expression in the developing and adult mouse inner ear. Stem Cells Dev. 2016 Oct
788 1;25(19):1419-32. PMID: 27474107.
789 43) Oiticica J, Barboza-Junior LCM, Batissoco AC, Lezirovitz K, Mingroni-Netto RC,
790 Haddad LA, et al. Retention of progenitor cell phenotype in otospheres from guinea pig and
791 mouse cochlea. J Transl Med. 2010 Nov 18;8:119. PMID: 21087511.
792 44) Li H, Roblin G, Liu H, Heller S. Generation of hair cells by step wise differentiation of
793 embryonic stem cells. Proc Natl Acad Sci USA. 2003 Nov 11;100(23):13495-500. PMID:
794 14593207.
795 45) Malgrange B, Belachew S, Thiry M, Nguyen L, Rogister B, Alvarez ML, et al.
796 Proliferative generation of mammalian auditory hair cells in culture. Mech Dev. 2002
797 Mar;112(1-2):79-88. PMID: 11850180.
798 46) Watanabe R, Morell MH, Miller JM, Kanicki AC, O'Shea KS, Altschuler RA, et al.
799 Nestin-expressing cells in the developing, mature and noise-exposed cochlear epithelium.
800 Mol Cell Neurosci. 2012 Feb;49(2):104-9. PMID: 22122823.

801 47) Lou X, Dong Y, Xie J, Wang X, Yang L, Tokuda M, et al. Comparing the cultivated
802 cochlear cells derived from neonatal and adult mouse. J Transl Med. 2014 May 29;12:150.
803 PMID: 24884939.
804 48) Hasson T, Heintzelman MB, Santos-Sacchi J, Corey DP, Mooseker MS. Expression of
805 cochlea and retina of myosin VIIa, the gene product defective in Usher syndrome type 1B.
806 Proc Natl Acad Sci USA. 1995 Oct 10;92(21):9815-9. PMID: 7568224.
807 49) Hasson T, Gillespie PG, Garcia JA, MacDonald RB, Zhao Y, Yee AG, et al.
808 Unconventional myosins in inner ear sensory epithelia. J Cell Biol. 1997 Jun 16;137(6):1287-
809 307. PMID: 9182663.
810 50) Cyr JL, Bell AM, Hudspeth AJ. Identification with a recombinant antibody of an inner-
811 ear cytokeratin, a marker for hair-cell differentiation. Proc Natl Acad Sci USA. 2000 Apr
812 25;97(9):4908-13. PMID: 10758152.
813 51) Keller JP, Homma K, Duan C, Zheng J, Cheatham MA, Dallos P. Functional regulation
814 of the SLC26-family protein prestin by calcium/calmodulin. J Neurosci. 2014 Jan
815 22;34(4):1325-32. PMID: 24453323.
816 52) Park C, Thein P, Kalinec G, Kalinec F. HEI-OC1 cells as a model for investigating
817 prestin function. Hear Res. 2016 May;335:9-17. PMID: 26854618.
818 53) Adler HJ, Belyantseva IA, Merritt RC, Frolenkov GI Jr, Dougherty GW, Kachar B.
819 Expression of prestin, a membrane motor protein, in the mammalian auditory and vestibular
820 periphery. Hear Res. 2003 Oct;184(1-2):27-40. PMID: 14553901.
821 54) Chou YH, Bischoff JR, Beach D, Goldman RD. Intermediate filament reorganization
822 during mitosis is mediated by p34cdc2 phosphorylation of vimentin. Cell. 1990 Sep
823 21;62(6):1063-71. PMID: 2169348.
824 55) Yamasoba T, Kondo K. Supporting cell proliferation after hair cell injury in mature
825 guinea pig cochlea in vivo. Cell Tissue Res. 2006 Jul;325(1):23-31. PMID: 16525832.

826 56) Nygard AB, Jorgensen CB, Cirera S, Fredholm M. Selection of reference genes for gene
827 expression studies in pig tissue using SYBR green qPCR. BMC Mol Biol. 2007 Aug 15;8:67.
828 PMID: 17697375.

829

830

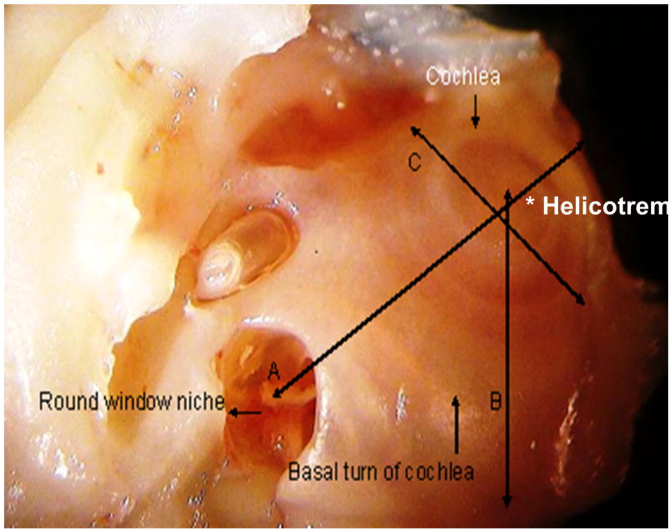
Cochlea
C
* Helicotrema
A
Round window niche
B
Basal turn of cochlea

A

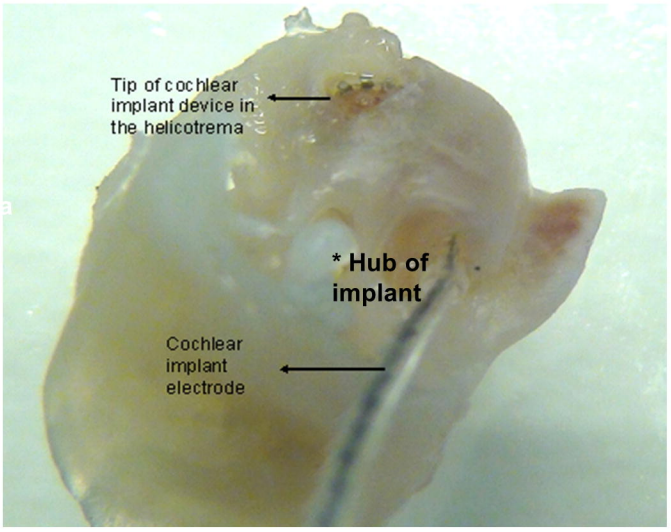
Tip of cochlear implant device in the helicotrema
* Hub of implant
Cochlear implant electrode

B

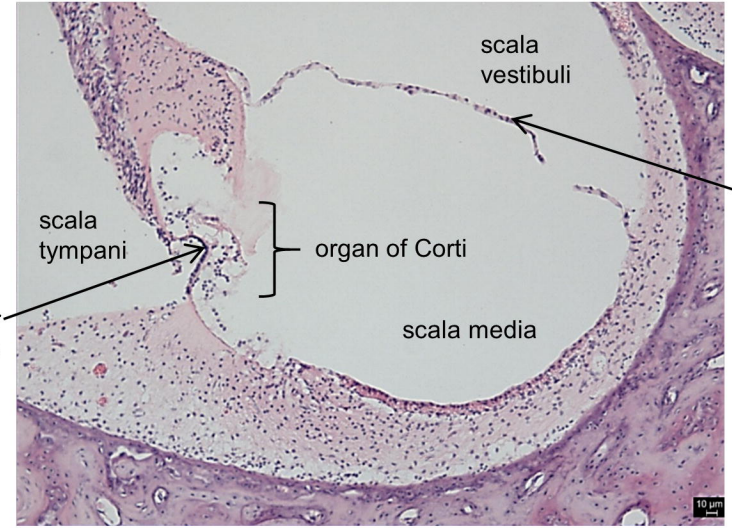
scala vestibuli
Reissner's membrane
scala tympani
organ of Corti
Basilar membrane
scala media
10 µm

C

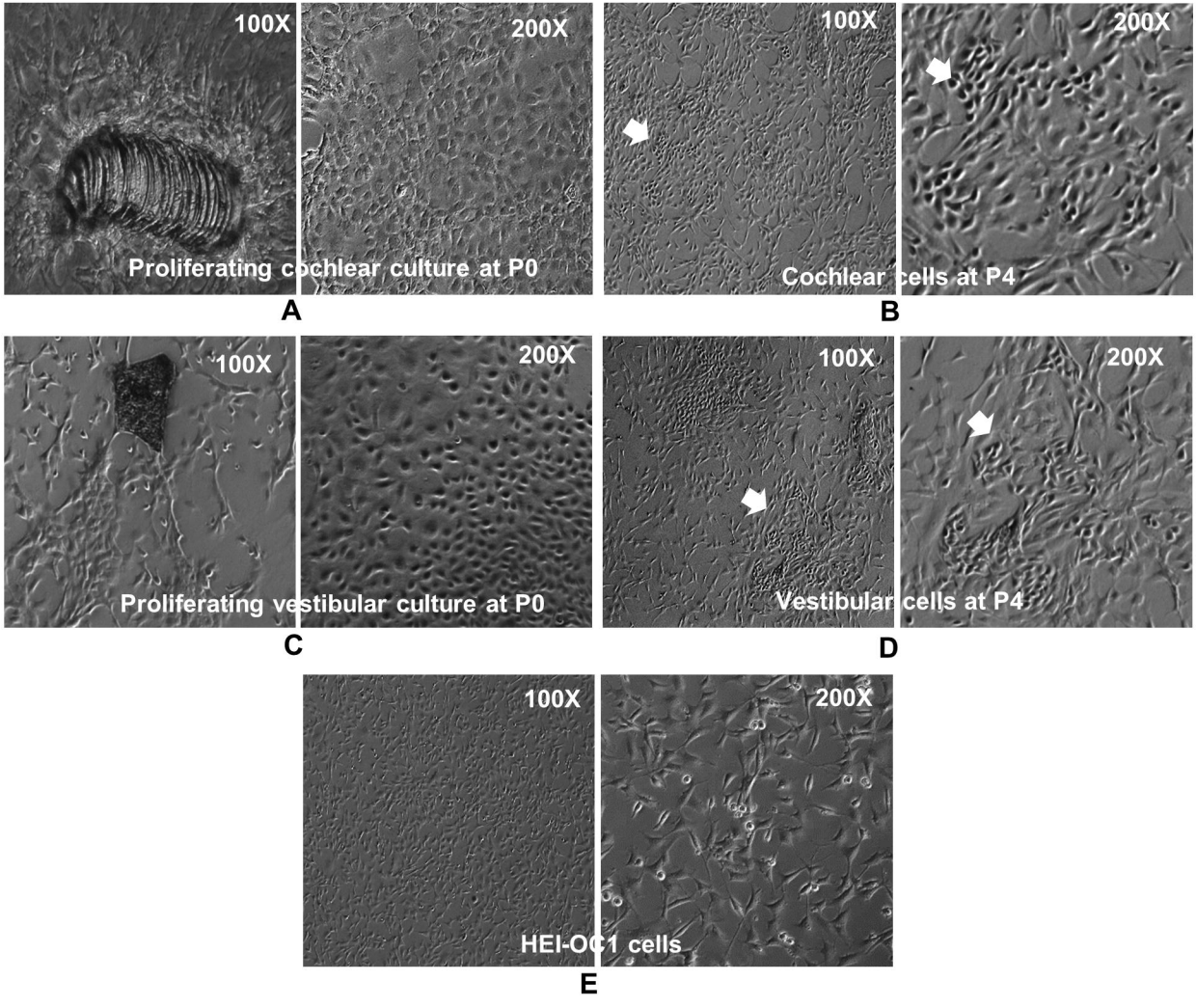
100X
200X
Proliferating cochlear culture at P0
A
100X
200X
Cochlear cells at P4
B
100X
200X
Proliferating vestibular culture at P0
C
100X
200X
Vestibular cells at P4
D
100X
200X
HEI-OC1 cells
E

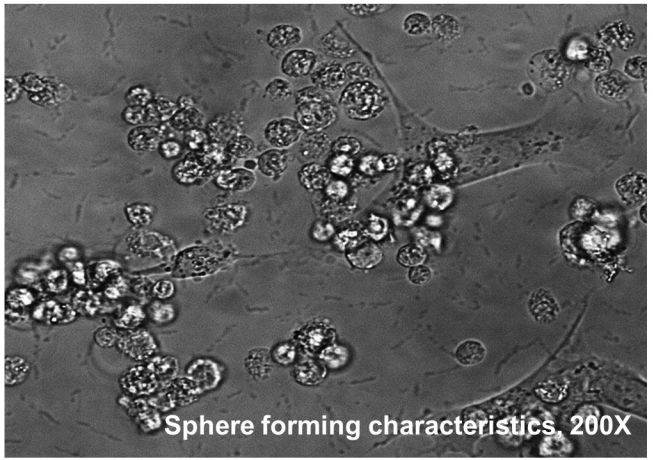
Sphere forming characteristics, 200X

A

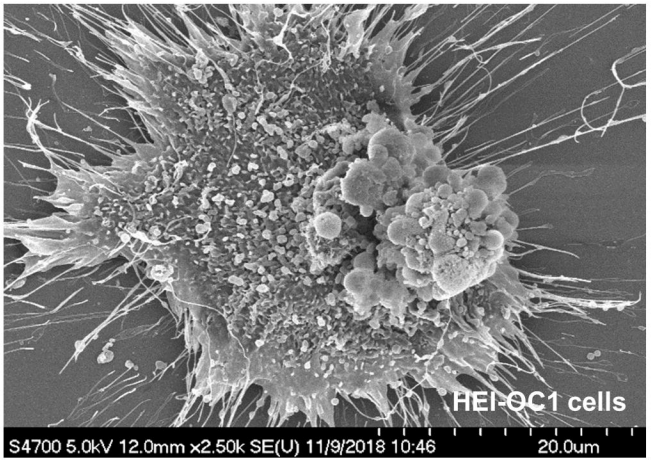
HEI-OC1 cells
S4700 5.0kV 12.0mm x2.50k SE(U) 11/9/2018 10:46
20.0um

B

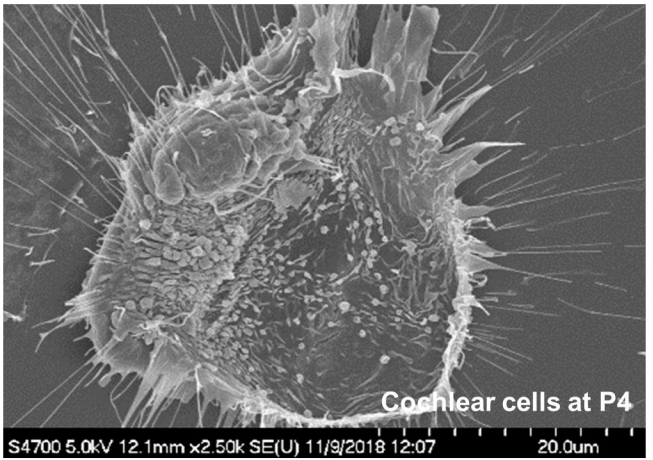
Cochlear cells at P4
S4700 5.0kV 12.1mm x2.50k SE(U) 11/9/2018 12:07
20.0um

C

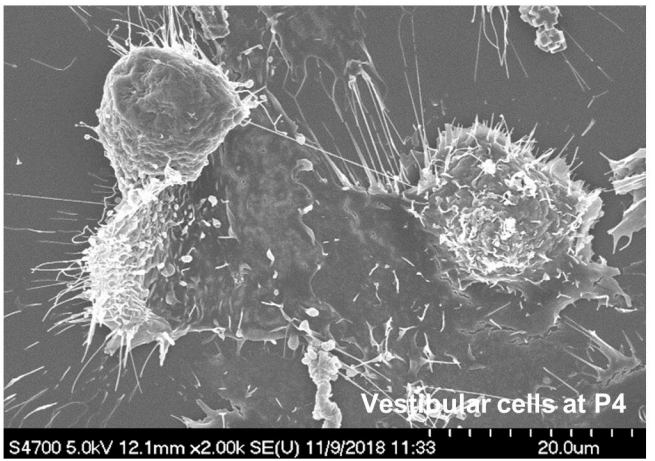
Vestibular cells at P4
S4700 5.0kV 12.1mm x2.00k SE(U) 11/9/2018 11:33
20.0um

D

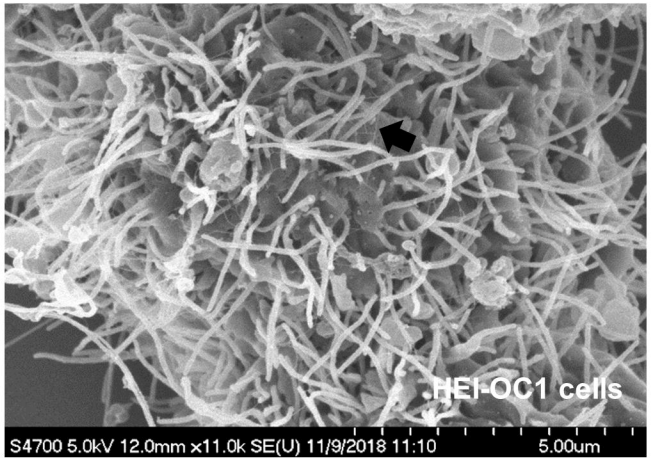
HEI-OC1 cells
S4700 5.0kV 12.0mm x11.0k SE(U) 11/9/2018 11:10
5.00um

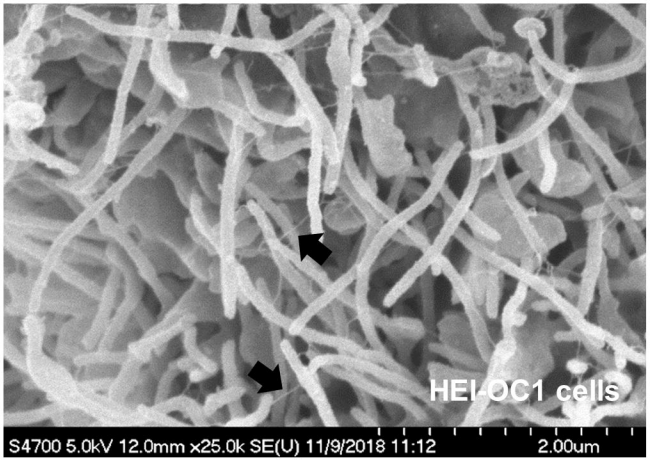
HEI-OC1 cells
S4700 5.0kV 12.0mm x25.0k SE(U) 11/9/2018 11:12
2.00um

A

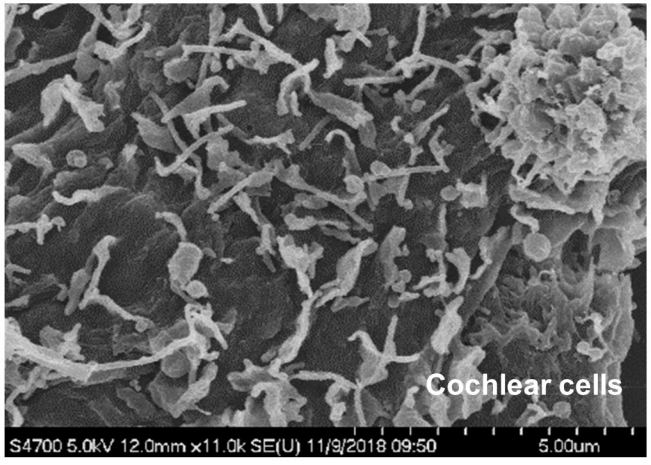
Cochlear cells
S4700 5.0kV 12.0mm x11.0k SE(U) 11/9/2018 09:50
5.00um

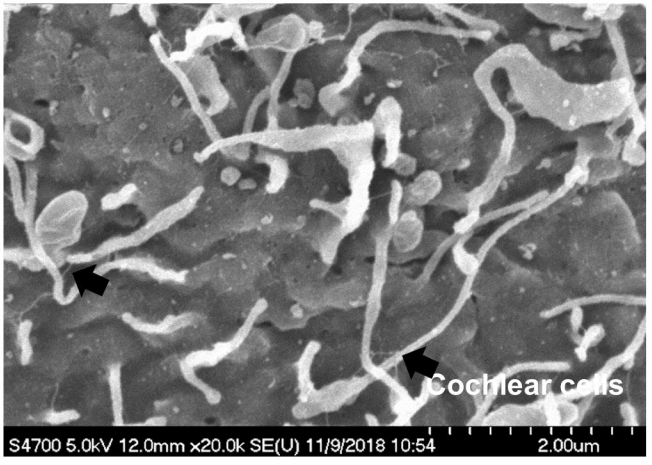
Cochlear cells
S4700 5.0kV 12.0mm x20.0k SE(U) 11/9/2018 10:54
2.00um

B

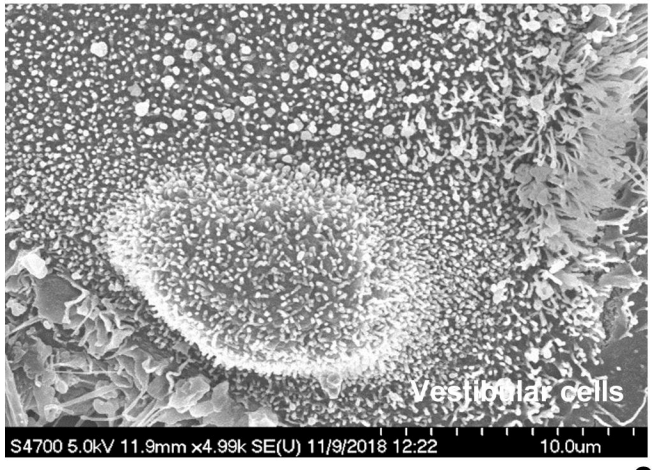
Vestibular cells
S4700 5.0kV 11.9mm x4.99k SE(U) 11/9/2018 12:22
10.0um

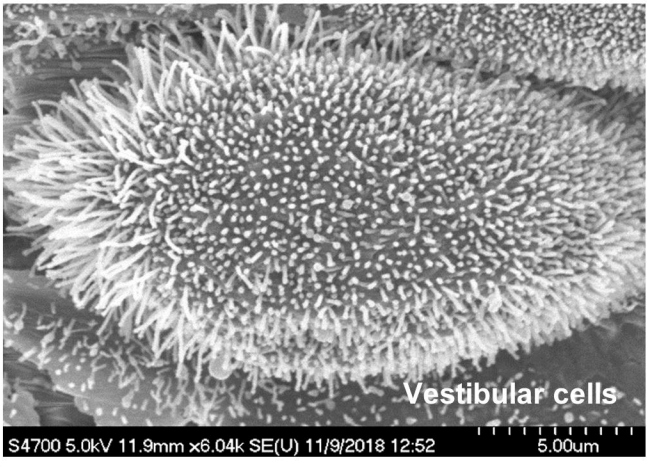
Vestibular cells
S4700 5.0kV 11.9mm x6.04k SE(U) 11/9/2018 12:52
5.00um

C

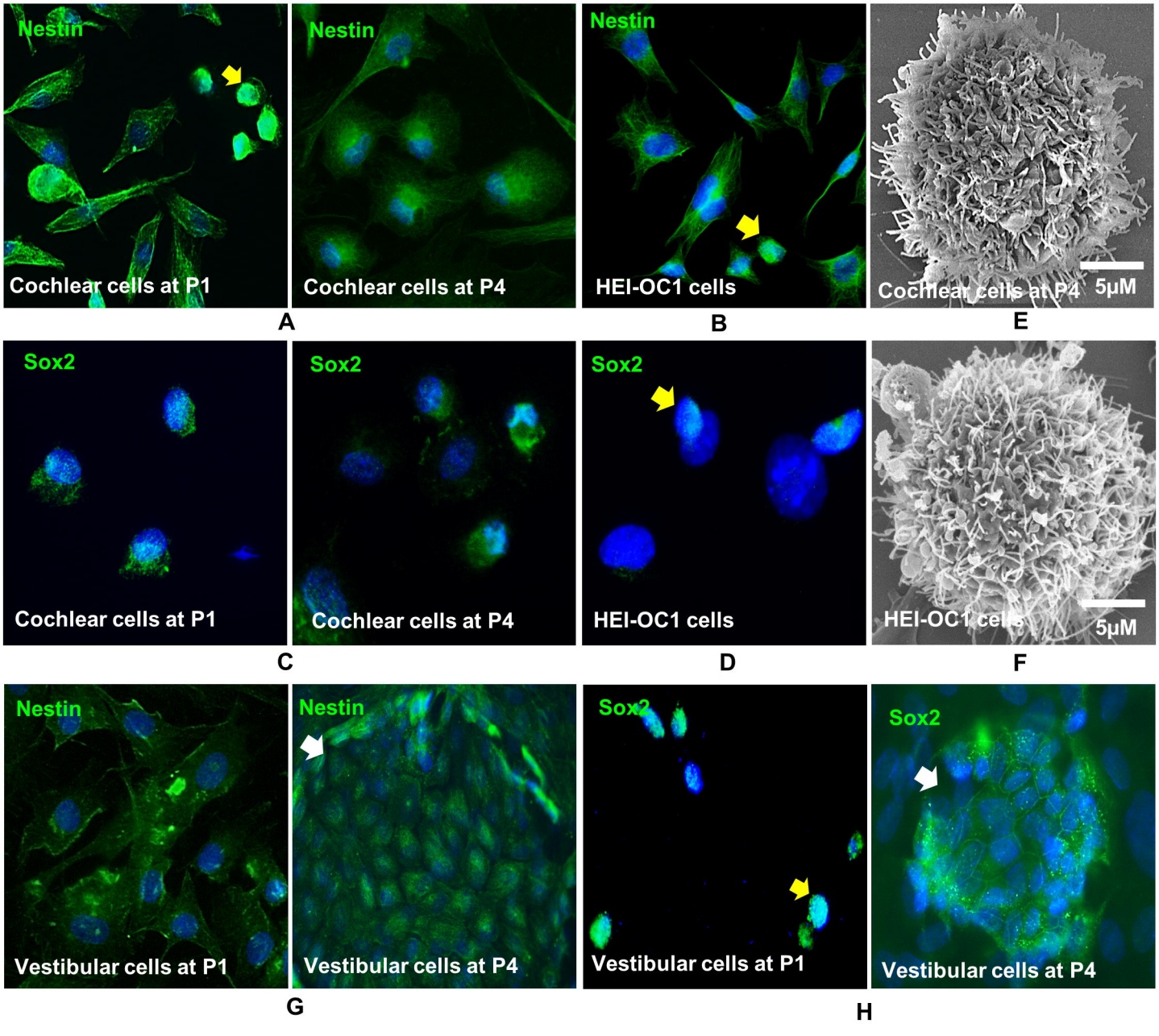
Nestin
Cochlear cells at P1
Nestin
Cochlear cells at P4
Nestin
HEI-OC1 cells
Cochlear cells at P4
5μM
A
B
E
Sox2
Cochlear cells at P1
Sox2
Cochlear cells at P4
Sox2
HEI-OC1 cells
HEI-OC1 cells
5μM
C
D
F
Nestin
Vestibular cells at P1
Nestin
Vestibular cells at P4
Sox2
Vestibular cells at P1
Sox2
Vestibular cells at P4
G
H

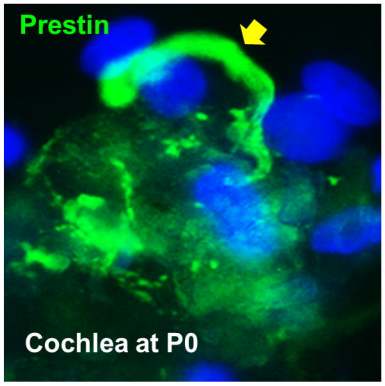
Prestin
Cochlea at P0

A

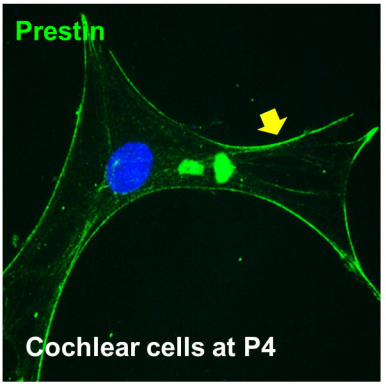
Prestin
Cochlear cells at P4

B

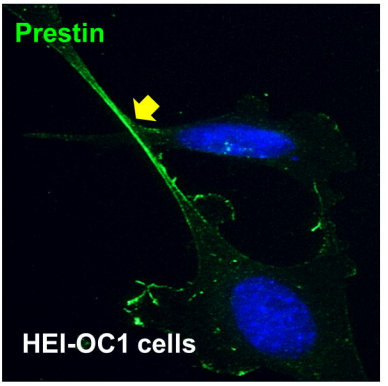
Prestin
HEI-OC1 cells

C

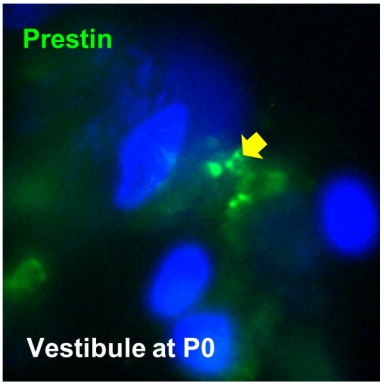
Prestin
Vestibule at P0

D

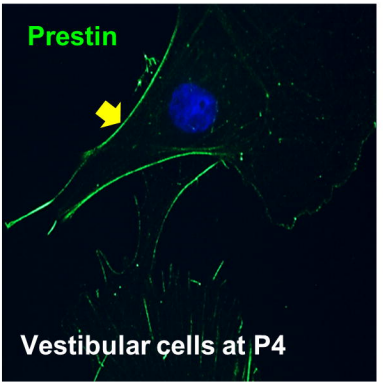
Prestin
Vestibular cells at P4

E

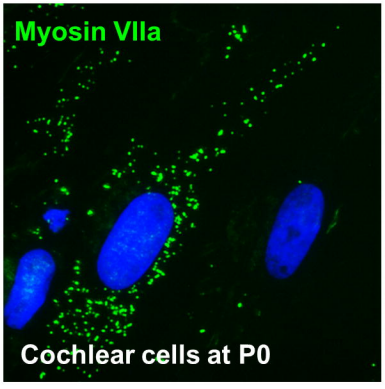
Myosin VIIa
Cochlear cells at P0

F

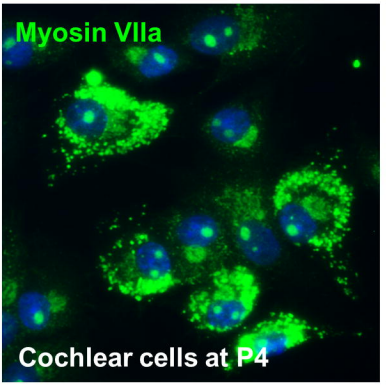
Myosin VIIa
Cochlear cells at P4

G

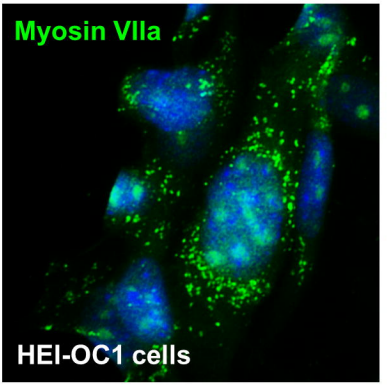
Myosin VIIa
HEI-OC1 cells

H

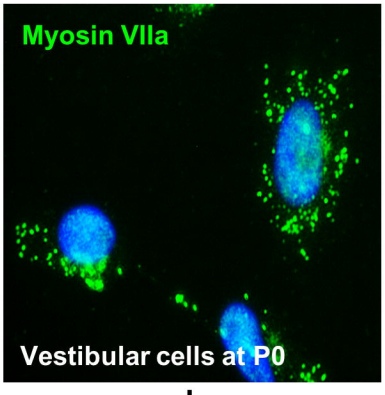
Myosin VIIa
Vestibular cells at P0

I

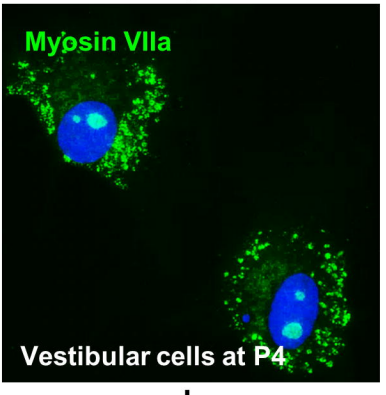
Myosin VIIa
Vestibular cells at P4

J

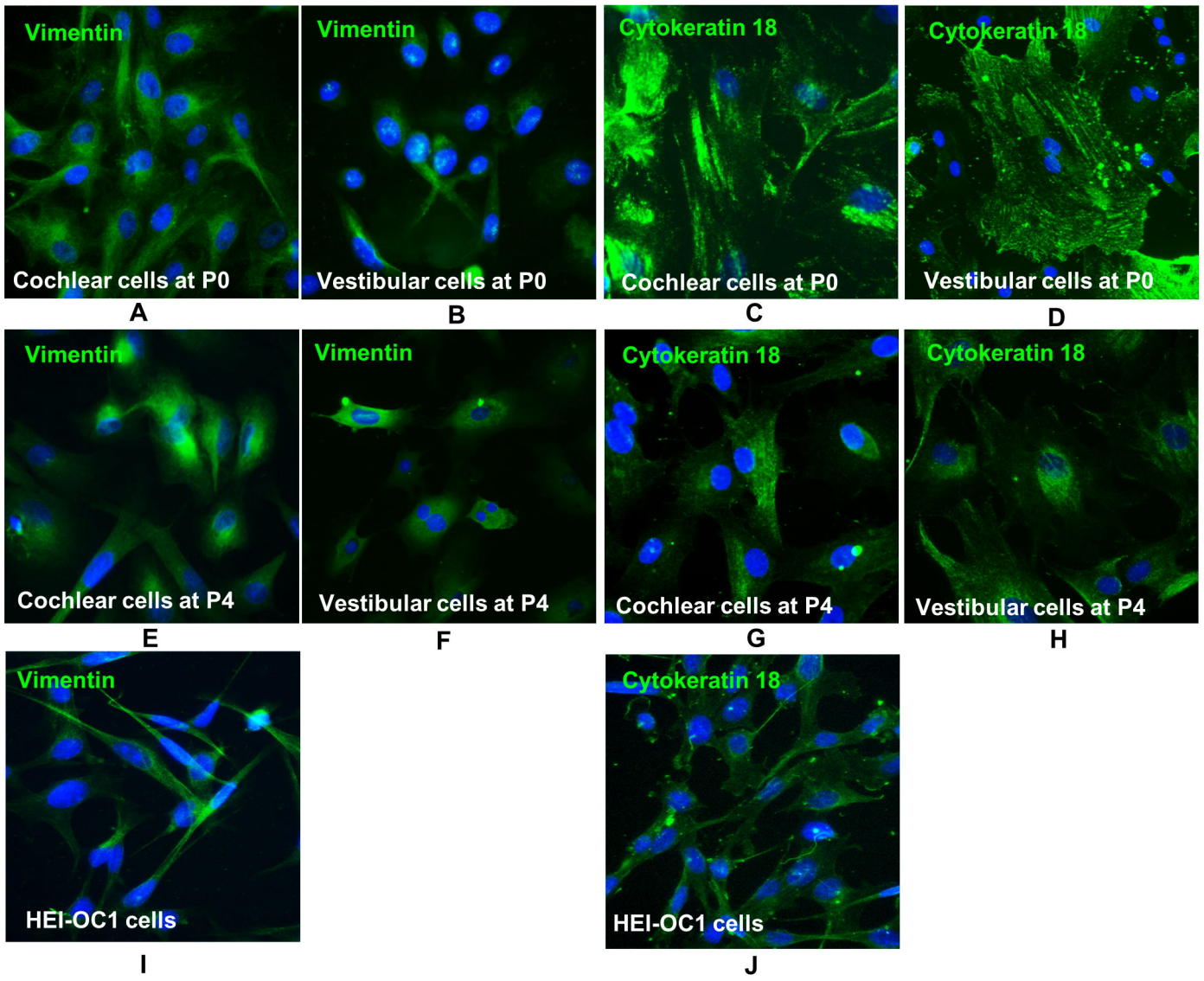
Vimentin
Cochlear cells at P0
A
Vimentin
Vestibular cells at P0
B
Cytokeratin 18
Cochlear cells at P0
C
Cytokeratin 18
Vestibular cells at P0
D
Vimentin
Cochlear cells at P4
E
Vimentin
Vestibular cells at P4
F
Cytokeratin 18
Cochlear cells at P4
G
Cytokeratin 18
Vestibular cells at P4
H
Vimentin
HEI-OC1 cells
I
Cytokeratin 18
HEI-OC1 cells
J

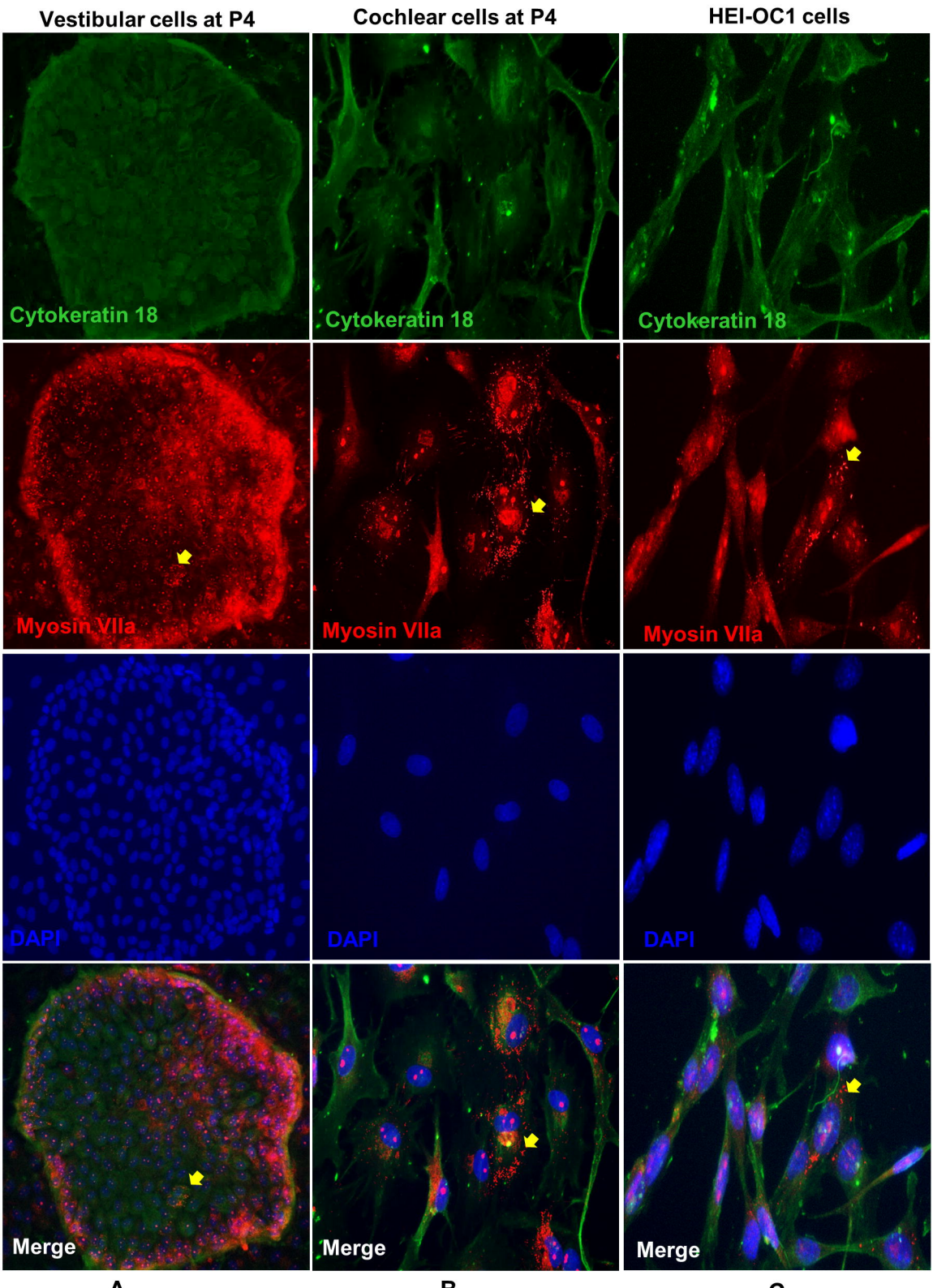
Vestibular cells at P4
Cochlear cells at P4
HEI-OC1 cells
Cytokeratin 18
Cytokeratin 18
Cytokeratin 18
Myosin VIIa
Myosin VIIa
Myosin VIIa
DAPI
DAPI
DAPI
Merge
Merge
Merge
A
B
C

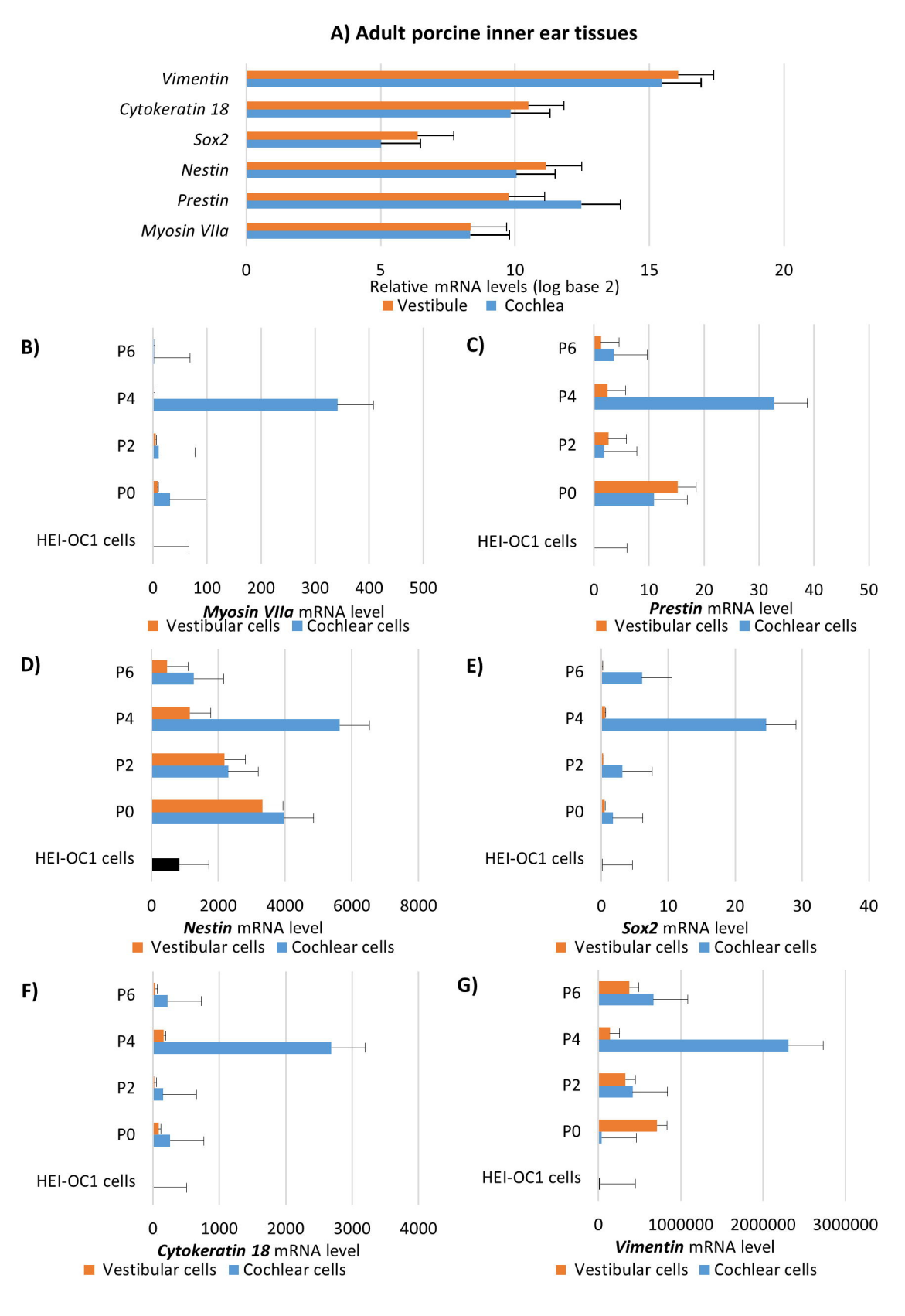
A) Adult porcine inner ear tissues
Vimentin
Cytokeratin 18
Sox2
Nestin
Prestin
Myosin VIIa
0
5
10
15
20
Relative mRNA levels (log base 2)
Vestibule
Cochlea
B)
P6
P4
P2
P0
HEI-OC1 cells
0
100
200
300
400
500
Myosin VIIa mRNA level
Vestibular cells
Cochlear cells
C)
P6
P4
P2
P0
HEI-OC1 cells
0
10
20
30
40
50
Prestin mRNA level
Vestibular cells
Cochlear cells
D)
P6
P4
P2
P0
HEI-OC1 cells
0
2000
4000
6000
8000
Nestin mRNA level
Vestibular cells
Cochlear cells
E)
P6
P4
P2
P0
HEI-OC1 cells
0
10
20
30
40
Sox2 mRNA level
Vestibular cells
Cochlear cells
F)
P6
P4
P2
P0
HEI-OC1 cells
0
1000
2000
3000
4000
Cytokeratin 18 mRNA level
Vestibular cells
Cochlear cells
G)
P6
P4
P2
P0
HEI-OC1 cells
0
1000000
2000000
3000000
Vimentin mRNA level
Vestibular cells
Cochlear cells